Redox Biology 46 (2021) 102067

Contents lists available at ScienceDirect

Redox Biology

journal homepage: www.elsevier.com/locate/redox

CCL5 via GPX1 activation protects hippocampal memory function after mild traumatic brain injury

Man-Hau Ho [a,b,c,d], Chia-Hung Yen [d], Tsung-Hsun Hsieh [e,f], Tzu-Jen Kao [a,b], Jing-Yuan Chiu [b], Yung-Hsiao Chiang [g,h,i], Barry J. Hoffer [a,b,i,j,k], Wen-Chang Chang [c], Szu-Yi Chou [a,b,*]

[a] Ph.D. Program for Neural Regenerative Medicine, College of Medical Science and Technology, Taipei Medical University and National Health Research, Taiwan
[b] Graduate Institute of Neural Regenerative Medicine, College of Medical Science and Technology, Taipei Medical University, Taipei, Taiwan
[c] Graduate Institute of Medical Sciences, College of Medicine, Taipei Medical University, Taipei, 11031, Taiwan
[d] Department of Biological Science and Technology, National Pingtung University of Science and Technology, Neipu, Pingtung, 91201, Taiwan
[e] School of Physical Therapy and Graduate Institute of Rehabilitation Science, Chang Gung University, Taoyuan, Taiwan
[f] Neuroscience Research Center, Chang Gung Memorial Hospital, Linkou, Taoyuan, Taiwan
[g] Department of Surgery, School of Medicine, College of Medicine, Taipei Medical University, 11031, Taiwan
[h] Department of Neurosurgery, Taipei Medical University Hospital, Taipei, 11031, Taiwan
[i] Neuroscience Research Center, Taipei Medical University, Taipei, 11031, Taiwan
[j] Department of Neurosurgery, Case Western Reserve University School of Medicine, Cleveland, OH, USA
[k] Scientist Emeritus, National Institutes of Health, USA

ARTICLE INFO

Keywords:
CCL5
Reactive oxygen species (ROS)
NADPH oxidase
Traumatic brain injury
Glutathione peroxidase - 1 (GPX1)

ABSTRACT

Traumatic brain injury (TBI) is a prevalent head injury worldwide which increases the risk of neurodegenerative diseases. Increased reactive oxygen species (ROS) and inflammatory chemokines after TBI induces secondary effects which damage neurons. Targeting NADPH oxidase or increasing redox systems are ways to reduce ROS and damage. Earlier studies show that C–C motif chemokine ligand 5 (CCL5) has neurotrophic functions such as promoting neurite outgrowth as well as reducing apoptosis. Although CCL5 levels in blood are associated with severity in TBI patients, the function of CCL5 after brain injury is unclear. In the current study, we induced mild brain injury in C57BL/6 (wildtype, WT) mice and CCL5 knockout (CCL5-KO) mice using a weight-drop model. Cognitive and memory functions in mice were analyzed by Novel-object-recognition and Barnes Maze tests. The memory performance of both WT and KO mice were impaired after mild injury. Cognition and memory function in WT mice quickly recovered after 7 days but recovery took more than 14 days in CCL5-KO mice. FJC, NeuN and Hypoxyprobe staining revealed large numbers of neurons damaged by oxidative stress in CCL5-KO mice after mTBI. NADPH oxidase activity show increased ROS generation together with reduced glutathione peroxidase-1 (GPX1) and glutathione (GSH) activity in CCL5-KO mice; this was opposite to that seen in WT mice. CCL5 increased GPX1 expression and reduced intracellular ROS levels which subsequently increased cell survival both in primary neuron cultures and in an overexpression model using SHSY5Y cell. Memory impairment in CCL5-KO mice induced by TBI could be rescued by i.p. injection of the GSH precursor – *N*-acetylcysteine (NAC) or intranasal delivery of recombinant CCL5 into mice after injury. We conclude that CCL5 is an important molecule for GPX1 antioxidant activation during post-injury day 1–3, and protects hippocampal neurons from ROS as well as improves memory function after trauma.

1. Introduction

Traumatic brain injury (TBI) is a prevalent cause of damage to the brain. The causes of TBI include vehicular accidents, blast during war, contact sports, and assaults. Injuries can range from mild concussions to severe permanent brain damage. Brain injuries can result in both physical and mental dysfunction. Brain trauma usually involves two different facets: first global injuries such as diffuse axonal injury which often leads an overall decreased level of consciousness; and second, focal injuries from which symptoms are based on the brain area affected. Secondary injury includes blood–brain barrier (BBB) damage, reactive

* Corresponding author. Ph.D. Program for Neural Regenerative Medicine, Graduate Institute of Neural Regenerative Medicine, College of Medical Science and Technology, Taipei Medical University, 250 Wu-Xing Street, Taipei City, 110, Taiwan.
E-mail addresses: sichou@tmu.edu.tw, sichou@gmail.com (S.-Y. Chou).

https://doi.org/10.1016/j.redox.2021.102067
Received 3 May 2021; Received in revised form 12 June 2021; Accepted 8 July 2021
Available online 17 July 2021

oxygen species (ROS) generation and free radical overload, increased inflammatory factors, excessive excitotoxicity from glutamate release, IL-10 expression in vascular smooth muscle cells and mouse brain [14,15]; IL-10 also promotes type-2 microglial differentiation and prevents

Abbreviations

AD	Alzheimer's disease
Aβ	Amyloid beta
BBB	blood–brain barrier
CCL5	Chemokine (C–C motif) ligand 5
CA1	hippocampus Cornu Ammonis areas 1
CPS	Counts per second
DAPI	4′,6-diamidino-2-phenylindole
Dpi	Days post injury
FJC staining	Fluoro-Jade C staining
GAPDH	Glyceraldehyde-3-phosphate dehydrogenase
GCS	Glasgow Coma Scale
GPX	Glutathione peroxidase
GS	Glutathione synthase
GSH	Glutathione
GSSG	Glutathione disulfide
H_2DCFDA	2′,7′-dichlorodihydrofluorescein diacetate
Hyproxprobe	Pimonidazole hydrochloride
HRP	Horseradish peroxidase
i.p.	Intraperitoneal injection
IL-1ß	Interleukin-1ß
LM	Long-term memory recall test
mTBI	Mild traumatic brain injury
MTT assay	3-(4,5-Dimethylthiazol-2-yl)-2,5-diphenyltetrazolium bromide assay
NAC	*N*-Acetyl-L-cysteine
NOR	Novel object recognition test
NOS	Nitric oxide synthases
NOX	Nicotinamide adenine dinucleotide phosphate (NADPH) oxidase
RANTES	Regulated on activation, normal T cell expressed and secreted
ROS	Reactive oxygen species
SM	Short-term memory recall test
SOD	Superoxide dismutase
TNF-α	Tumor necrosis factor-alpha
Tuj-1	Neuron-specific class iii beta-tubulin

and dysfunction of mitochondrial activity in neurons.

Inflammatory reactions and increased oxidative stress (OS) are two major causes of secondary injury after TBI. Traumatic brain injury and NADPH oxidase are highly correlated [1,2]. Studies here found that NOX2 expression and NADPH oxidase activity increase rapidly in the mouse cerebral cortex and hippocampal CA1 region in TBI animals. NADPH oxidase activity increases with an early peak at 1 h in neurons, followed by a secondary peak from 24 to 96 h after TBI in microglia. NADPH oxidase generates super dioxide ($O2^-$) which is further converted into H_2O_2 by SOD (Superoxide dismutase). Both super dioxide and H_2O_2 are highly reactive molecules which oxidize cellular proteins or lipids and increase oxidative stress. O_2 binding with reduced (Fe^{2+}) heme proteins generates an Fe (III) superoxide complex. Some studies have targeted NADPH oxidase in order to reduce ROS generation for TBI therapy [3,4]. H_2O_2 can be converted into harmless H_2O and O_2 by the glutathione system -glutathione peroxidase (GPX) and reduced glutathione. When the cellular glutathione system (enzyme – GPX and glutathione) is reduced, the detoxification of oxygen metabolites will be rate-limited. NAC ((2,4-disulfonyl alpha-phenyl tertiary butyl nitrone and (*N*-acetyl L-cysteine)) is a precursor of glutathione, a thiol-rich agent, which can interact with reactive species and reduce cellular oxygen metabolites. Our previous study found significant improvement of TBI with *N*-acetylcysteine treatment [5,6]. Also, NAC treatment modulates the inflammatory status by activating M2 microglia rather than suppressing the immune reactions [7]. These suggest the importance of antioxidant activation and immune response balance for recovery after brain injury. Indeed, both preclinical and clinical studies have found positive effects of NAC in several TBI models, including the weight drop model used here [5,6,8,9].

Central repair systems and antioxidant activation in brain contribute to the outcome after brain injury; the immune system and chemokines released after TBI may participate in those process. The functions of many chemokines in brain trauma progression have been studied; however, the role of the chemokine CCL5 in brain injury is largely unknown. In both TBI animals and TBI patients, CCL5 mRNA is upregulated in the cortex after TBI [10,11]; CCL5 is also elevated in the plasma of TBI patients and its concentration at hospital admission may correlate with outcome in TBI patients [12,13]. Many studies suggest CCL5 has a protective role during neuronal damage. In particular, CCL5 upregulates pathological microglial hyperactivation [16,17]. Interestingly, studies have found that Alzheimer's disease (AD) patients have lower CCL5 levels in serum [18,19] and that CCL5 prevents Aβ toxicity in neurons both with *in vitro* and *in vivo* studies [20,21]. In a chemokine array study, increased CCL5 and CCR5 was found after stroke; moreover, more neuronal loss was seen in CCL5 deficient mice after stroke [22]. CCL5 was also found to be essential for stem cell therapy in an AD model; AD mice receiving bone marrow mesenchymal stem cell transplantation from CCL5 deficient mice failed to recovery memory [20]. Our laboratory has also shown that CCL5 is an important factor contributing to neurite growth and memory formation [15]. Taken together, these studies suggest that CCL5 might be an important factor for modulating inflammatory processes and preventing neuronal death after brain damage.

In this current study, we induced mild brain injury in C57BL/6 (wildtype, WT) mice and CCL5 knockout (CCL5-KO) mice using a weight-drop model. Cognitive and memory functions in mice were analyzed by Novel-object-recognition and Barnes Maze tests. The memory performance of both WT and KO mice were impaired after mild injury. Cognition and memory function in WT mice quickly recovered after 7 days but recovery took more than 14 days in CCL5-KO mice. FJC, NeuN and Hypoxyprobe staining revealed large numbers of neurons damaged by oxidative stress in CCL5-KO mice after mTBI. NADPH oxidase activity indicated increased reactive oxidative species (ROS) generation with reduced GPX1 protein and GSH activity in CCL5-KO mice which was opposite to that seen in WT mice. CCL5 increased GPX1 expression and reduced intracellular ROS levels which increased cell survival both in primary neuron cultures and in an overexpression model using a SHSY5Y cell line. Memory impairment in CCL-KO mice induced by TBI could be rescued by i.p. injection of the GSH precursor – NAC and intranasal delivery of CCL5 recombinant protein into mice after injury.

2. Results

2.1. Memory recovery was delayed in CCL5 deficiency mice after mild brain injury

Both wild-type (WT) and CCL5-knockout (CCL5-KO) mice were

subjected to mild brain injury at 2-months of age with the weight-drop system. The unconsciousness time (righting reflex) was increased in both types of mice after weight-drop-induced brain trauma and there was no difference between these two groups of animals (Supl. Fig. 1A). The modified neurological severity score (mNSS) was used to evaluate the injury. The mNSS was about 3, showing mild injury, in both WT and CCL5-KO mice one day after injury (Supl. Fig. 1B). Novel object recognition (NOR) and the Barnes maze (BM) were used to analyze short-term recognition memory and spatial memory in these mice (Fig. 1A). The preference for new objects was not different between WT and CCL5-KO groups without injury. The preference for new objects was reduced after mild brain injury and started to recover after 7 days in the WT group but only after 14 days in CCL5-KO group (Fig. 1B). Locomotor ability in both groups of mice was not affected (Fig. 1C). The primary latency in short-term memory recall (SM, 2 days after training) and long-term memory recall (LM, 7 days after training) in the Barnes maze was similar in both WT and CCL5-KO mice sham and mTBI groups before injury; the primary latency in the recall test was increased in both mTBI groups after injury for 2 days (2 days-recall) (Fig. 1D and E). WT mice recovered from the TBI-induced mnemonic loss quickly; the primary latency for new BM learning and memory tests at post injury (dpi) day 4 (Fig. 1F and 4 dpi) or day 28 (Figs. 1G and 28 dpi) was not different between sham and injury WT groups. The memory recall tests and walking path distance was also not different between sham and TBI groups in WT animals (Supl. Fig. 2A–D). In contrast, the primary latency in the mouse KO TBI group was higher at 4 days post injury (dpi) in the BM compared to sham (Fig. 1F), and was even higher at 28 dpi in the BM (Fig. 1G; *, $p = 0.0432$ comparing KO-TBI 28 dpi to 4 dpi BM in 1F by two-way ANOVA; $p = 0.0353$ in trial 4 of KO-TBI at 28 dpi and 4 dpi BM in 1F by *t*-test). The primary latency and walking path for short-term memory recall was increased in the KO TBI group (Supl. Fig. 2E–H) but was also not different between sham and TBI groups in WT animals.

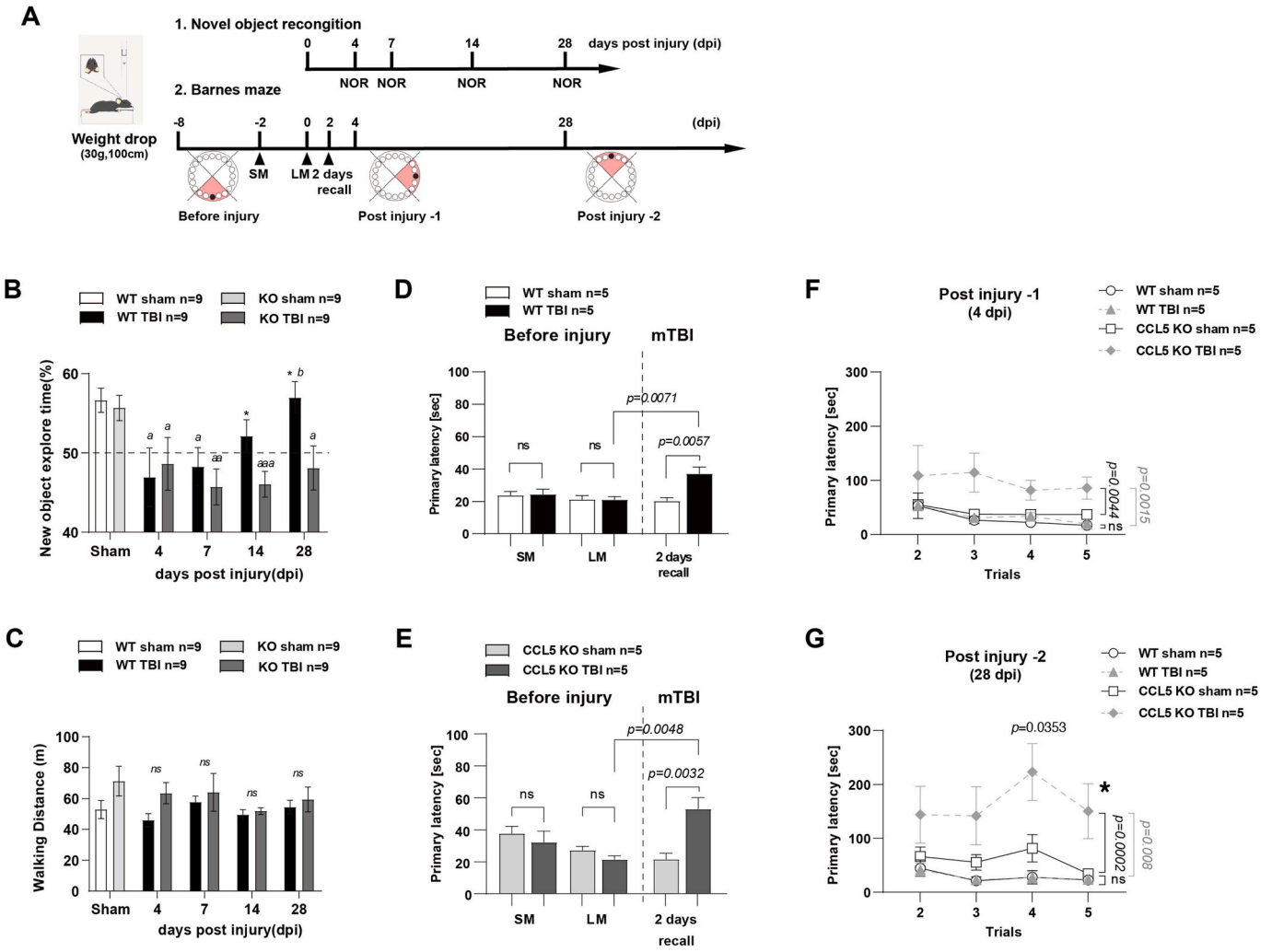

Fig. 1. Memory impairment and recovery in WT and CCL5-KO mice after mTBI. (A) The time table of experimental design for mild TBI induction and memory-cognition function tests – novel object recognition (NOR) and Barnes maze (BM). (B) The preference index of WT and KO mice for new objects in sham and mTBI groups after weight-drop induced mild TBI. Tests were performed on post injury days 4 , 7 , 14 , and 28. (a , $p < 0.05$, aa , $p < 0.01$, aaa , $p < 0.001$ compared to sham group with *t*-test; b, $p < 0.05$, WT 28 days compared to 7 days; * , $p < 0.05$, WT compared to KO at the same time point with *t*-test.) (C) The walking path length in WT and KO mice. (ns: no significant difference). Data is shown as mean ± S.E.M ($n = 9$ for each group). Spatial memory was analyzed by Barnes maze as the latency to reach the shelter box (Primary latency). (D, E) Recall memory was performed after 2 days (short-term, SM), 7 days (long-term, LM) of training and 2 days after weight-drop induced TBI. (F–G) New learning-memory tasks were taken after 4 days and 28 days of injury. Data was analyzed by Two-way ANOVA and presented as mean ± S.E.M. (*, $p = 0.0432$ compared to KO-TBI 4 dpi BM in 1F by two-way ANOVA; $p = 0.0353$ in Trial 4 compare to KO-TBI 4 dpi BM in 1F by *t*-test.) ($n = 5$, in each group).

2.2. The number of damaged neurons in hippocampus after mild trauma was increased in mice lacking CCL5

To examine the possible cause of memory impairment in CCL5-KO after trauma, we analyzed hippocampal neuron damage and neuron numbers 28 days after injury. FJC labeled damaged neurons in hippocampus increased in both WT and CCL5-KO mouse TBI groups but more FJC labeling was found in the KO TBI group compared to the WT TBI group (Fig. 2A, C). In addition, the number of hippocampal neurons labeled by NeuN was reduced in CCL5-KO mice 1-month after trauma (Fig. 2B, D) but not in WT animals. Moreover, inflammatory cells were not increased in WT mice 1-month after TBI since GFAP or Iba1 positive cells were similar between sham and TBI groups (Supl. Fig. 3); however, more astrogliosis, but not more microglia, were found in CCL5-KO mouse hippocampus after TBI (Supl. Fig. 3A, C and Supl. Fig. 3B, D). We also found increased TNF-α, IL-1β and IL-10 in WT mouse hippocampus after 4–7 dpi but this was reduced after 14 days. On the contrary, TNFα, IL-1β increased in KO mice at 14–28 dpi (Supl. 3E-G). These findings suggest a different modulation of immune responses in the KO mice after injury, especially for activation of IL-10, and that more neurons are lost and/or damaged in CCL5-KO mice after mild brain trauma together with increased astrogliosis. These findings are consistent with the behavioral performance data in Fig. 1. Taken together, recovery of hippocampal neurons from mild trauma appears reduced in mice lacking of CCL5.

2.3. CCL5 levels after early-stage trauma were correlated with neuronal oxidative stress

To further understand the association between CCL5 levels and neuron recovery after brain trauma, we analyzed the tissue levels of CCL5 by ELISA. The levels of CCL5 in hippocampal tissue increased after 4 dpi and gradually recovered after 14 dpi in WT mice (Supl. Fig. 4A); this is correlated with the timeline for memory recovery in WT mice. Oxidative stress is thought to be a major cause of neuron damage at early stages after brain trauma. Accordingly, cells under oxidative stress were labeled by hypoxyproble (green in Fig. 3) and co-labeled with either the neuron marker-NeuN (red in Fig. 3; also, Supl Fig. 5A) or the astrocyte marker - GFAP (red, Supl Fig. 5B). Hypoxyprobe-labeled cells were mostly NeuN positive but were not GFAP positive. The overall numbers of hippocampal neurons were not different between sham, 1 dpi and 7 dpi in both WT and KO mice (Fig. 3A–C, NeuN^{+}). Hypoxyprobe-labeled cells increased at 1 dpi and recovered to normal levels at 7 dpi in WT mice (Fig. 3A, D-hypoxyprobe^{+}), similar to the NeuN^{+} co-labeled cells

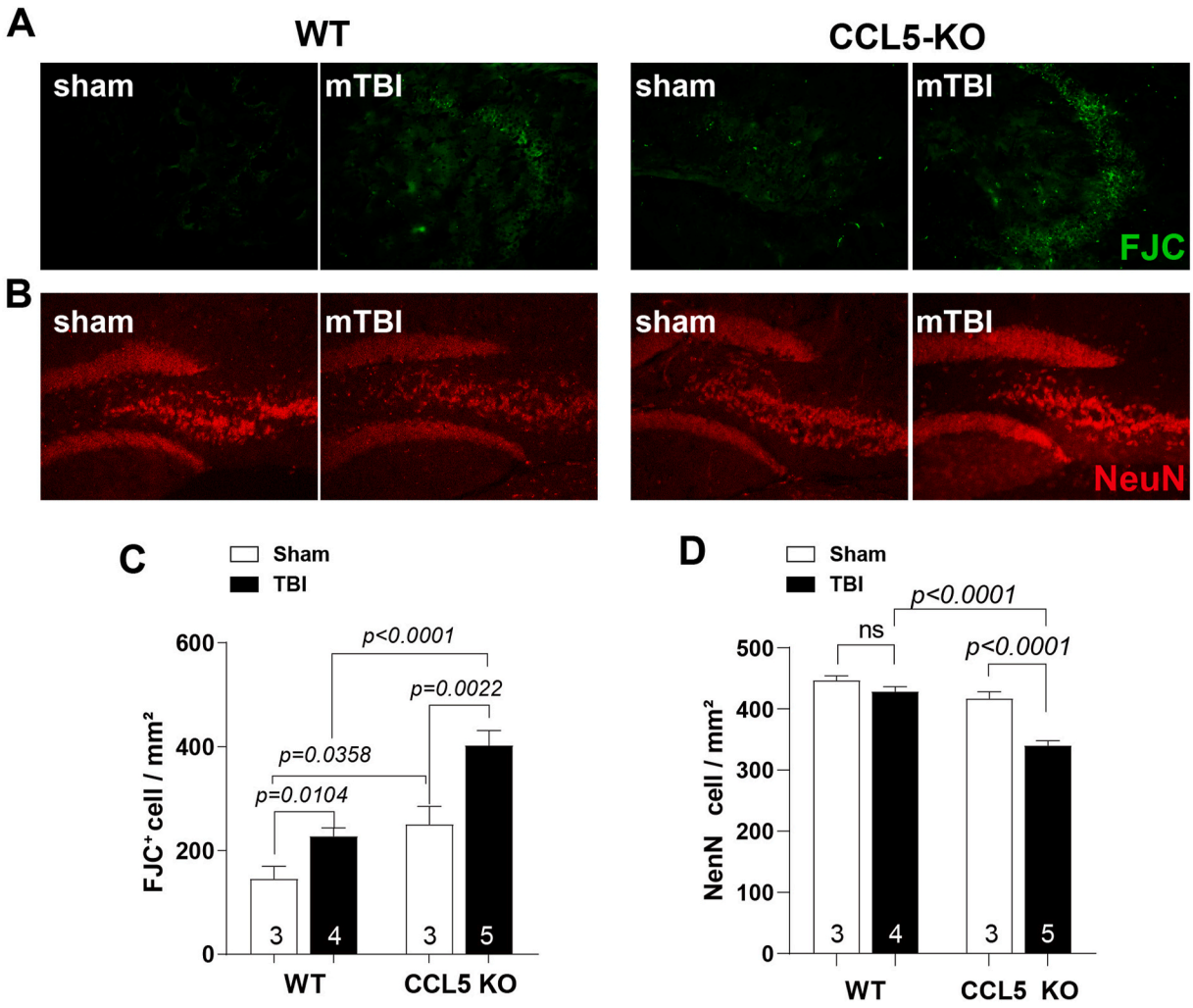

Fig. 2. Neuron damage and neuron numbers in hippocampus 28 days after injury. (A) Representative images of FJC labeling (green) in WT and CCL5-KO hippocampus. (C) Quantitation of FJC positive cells in WT and CCL5 KO mouse sham and mTBI groups. Increased FJC positive neurons were found in both mTBI groups. (n = 3 in each group). (B) Representative images of NeuN labeled (red) neurons in WT and CCL5-KO mouse hippocampus. (D) Quantitation of NeuN positive cells in different groups. NeuN positive neurons were significantly lower in the CCL5-KO mTBI group. (Data was analyzed by *t*-test and presented as mean ± S.E.M.) (n = 3–5 as showed in figures). Scale bar = 100 μm. (For interpretation of the references to color in this figure legend, the reader is referred to the Web version of this article.)

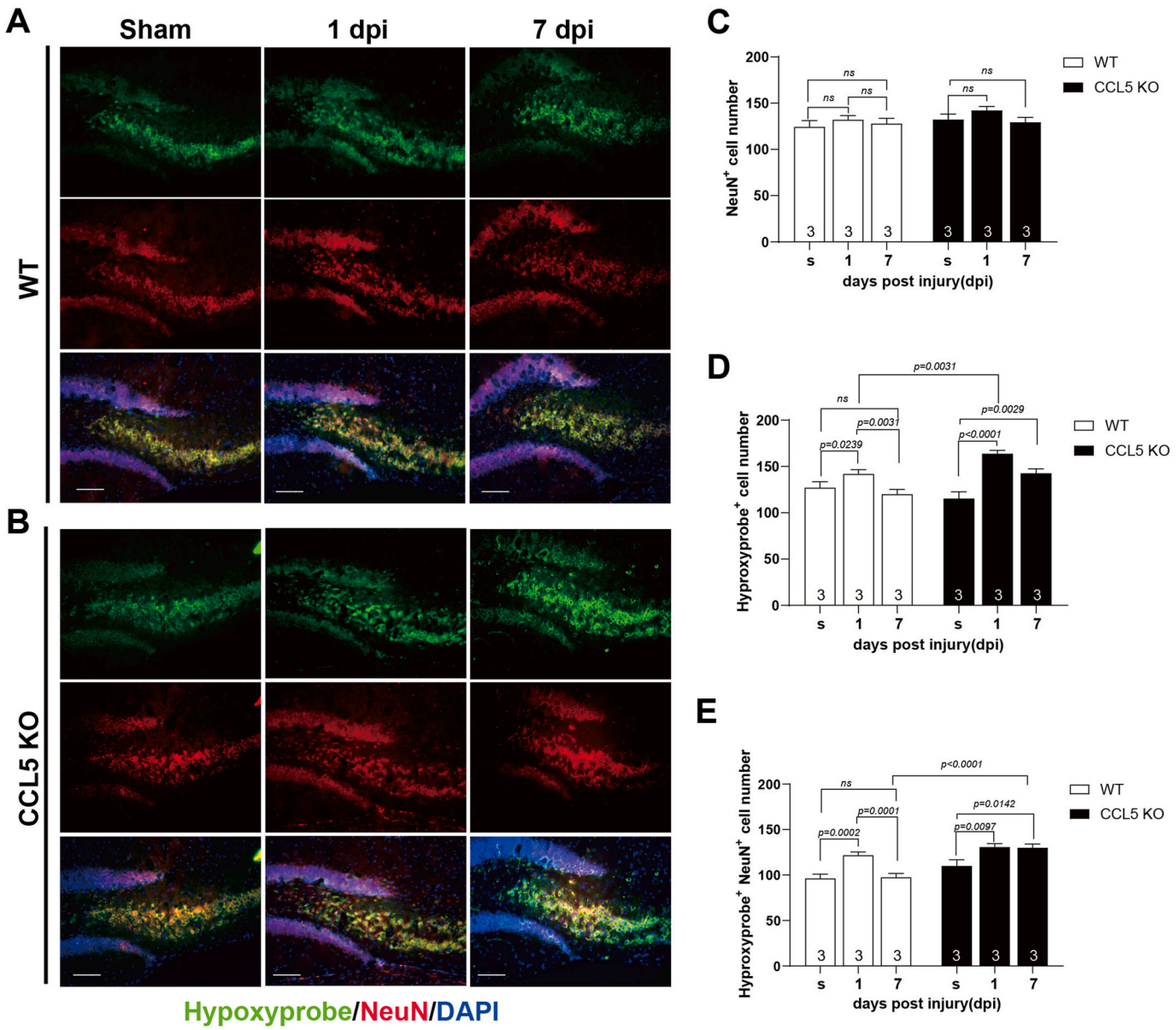

Fig. 3. Hypoxyprobe labeled hypoxic cells colocalized with NeuN positive neurons in WT and CCL5-KO mice at 1 day and 7 days post injury (dpi). Cells with hypoxia were labeled by hypoxyprobe (green) and neurons were labeled by NeuN (red) in both WT and CCL5-KO mice at 1 dpi and 7 dpi as well as sham treatment (s). (A–B) Representative images of hypoxylprobe and NeuN labeling in the hippocampal region of WT and CCL5-KO mice. (C–E) Quantitation of NeuN positive cells ($NeuN^+$, C), hypoxyprobe positive cells ($hypoxyprobe^+$, D) and both hypoxyprobe and NeuN positive cells ($hypoxyprobe^+NeuN^+$, E) at post injury day-1 and day-7 and sham in both WT and KO mice. (Data was analyzed by *t*-test and presented as mean ± S.E.M.) (n = 3 in each group). Scale bar = 100 μm. (For interpretation of the references to color in this figure legend, the reader is referred to the Web version of this article.)

(Fig. 3A, E-$hypoxyprobe^+$; $NeuN^+$). In contrast, increased numbers of hypoxyprobe labeled cells were seen at 1 dpi to 7 dpi in CCL5-KO mice (Fig. 3B, D-$hypoxyprobe^+$), especially in neurons (Fig. 3B, E-$hypoxyprobe^+$; $NeuN^+$). This suggests more neurons under oxidative stress are seen in CCL5-KO mice after trauma, since the increased oxidative stress at 1 dpi was reduced to normal after 7 dpi in WT mice but not in KO mice. Thus, CCL5 may play a critical role in neuronal oxidative stress status after trauma.

2.4. *Increased ROS generation and impaired activation of antioxidants in CCK5-KO mouse hippocampus after trauma*

Trauma induces NADPH oxidase activation and increases cellular ROS; O_2^- generated by NADPH oxidase can be converted to H_2O_2 by SOD and then be scavenged by the GPX system (Fig. 4A). Thus, we studied NADPH dependent ROS generation in mouse hippocampal tissue using a lucigenin assay (See Material and Methods). NADPH-generated ROS in hippocampal tissue was not significantly different between sham, and post injury 4- and 7-day WT mice but was significantly increased in CCL5-KO mice at post injury days 4 and 7 (Fig. 4B). The protein levels of the antioxidant GPX1, but not SOD1 and SOD2, were specifically increased in WT tissue 4 and 7 days after injury (Fig. 4C–F). In contrast, none of these antioxidant molecules increased after injury in CCL5-KO mouse hippocampus (Fig. 4C, G-I); we found reduced SOD1 protein in CCL5-KO hippocampus after 4 and 7 dpi (Fig. 4C, G). We further studied the function and activation of GPX1 between WT and CCL5-KO. GSH generation was lower in CCL5-KO tissue compared to WT (Fig. 4J); the reduced form GSH was also lower in CCL5-KO tissue (Fig. 4K) and the mRNA level of GPX1 in mouse hippocampus was also lower in the CCL5-KO mice (Fig. 4L). Expression of GPX1 mRNA increased after TBI in WT

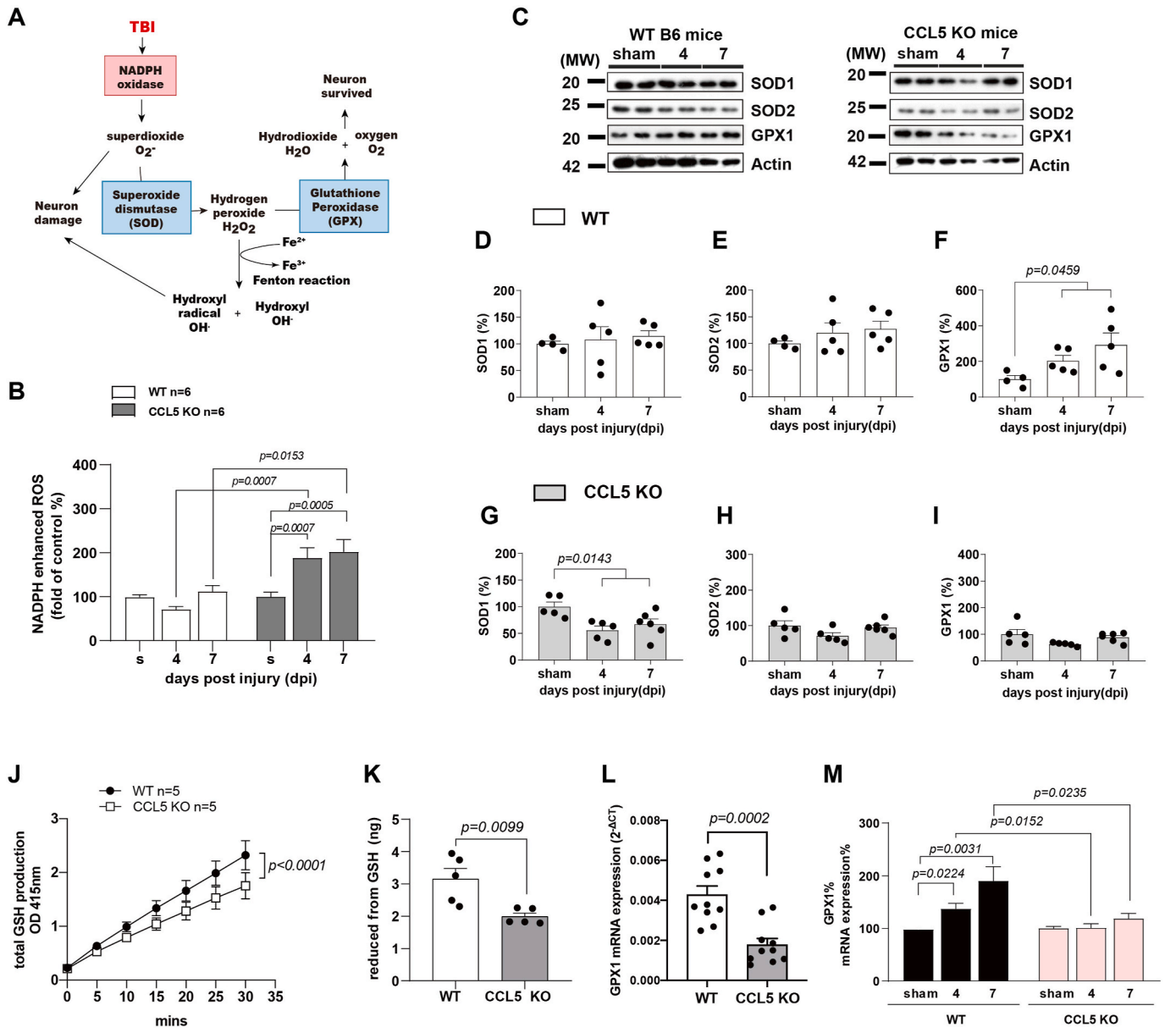

Fig. 4. NADPH and antioxidant activation in WT and CCL5-KO mouse hippocampus after mild TBI. (A) Reactive oxygen species generation induced by brain trauma and related antioxidants in the scavenger pathway. (B) NADPH oxidase activity in mouse hippocampus tissue was measured at 4 and 7 dpi compared to sham group in WT and CCL5-KO mice. (Data was analyzed by *t*-test and presented as mean ± S.E.M.); (n = 6 in each group). (C–I) The protein levels of antioxidants - SOD1, SOD2 and GPX1 in mouse hippocampus at 4 dpi and 7 dpi and sham groups were analyzed. (C) The representative images of SOD1, SOD2 and GPX1 protein blots in WT mice and CCL5-KO mice. Quantitative results of SOD1 (D, G), SOD2 (E, H) and GPX1 (F, I) in WT mice and CCL5-KO mice. (Data was analyzed by One-way ANOVA and presented as mean ± S.E.M.) (n = 5 in each group). (J–K) The total GSH production and reduced form of GSH were measured and were lower in CCL5-KO mice compared to WT mice. (Data was analyzed by two-way ANOVA in A and *t*-test in B. Data are presented as mean ± S.E.M.) Quantitative PCR analysis of GPX1 gene expression in WT and CCL5-KO mice control hippocampus (L) and mice with mTBI at 4 dpi and 7 dpi as well as in sham mice (M). (Data was analyzed by *t*-test and presented as mean ± S.E.M.)

mouse hippocampus; in contrast GPX1 was not activated in mice lacking CCL5 (Fig. 4M). This suggests that CCL5 might reduce tissue ROS levels through increasing the antioxidant – GPX1 under normal conditions; hippocampal tissue ROS increased, in contrast, in mice lacking of CCL5.

2.5. *Both intracellular and extracellular CCL5 protects neurons from ROS-induced cell death*

We further tested the protective effects of CCL5 in an *in vitro* culture system. Primary neurons expressing CCL5, or recombinant CCL5 when added into the culture, reduced cell death from H_2O_2 induced ROS (Fig. 5A and B). Intracellular ROS labeling by DCFDA was increased upon H_2O_2 treatment and was reduced by adding recombinant CCL5 to the primary neurons from KO mice except for a high dose (500 μM H_2O_2) which killed most of the neurons and for which added CCL5 failed to rescue them (Fig. 5C). Overexpressing CCL5 (Fig. 5F) in SHSY5Y cells also increased cell viability after H_2O_2 treatment (Fig. 5D). GPX1 protein levels increased when cells were treated with H_2O_2; interestingly, the basal cellular level of GPX1 protein increased after overexpressing CCL5 and GPX1 levels were still further increased after treatment with H_2O_2 (Fig. 5E). Additional recombinant CCL5 (10, 100 pg/ml) treatment increased GPX1 protein expression in the primary neurons' cultures from CCL5-KO (Fig. 5G).

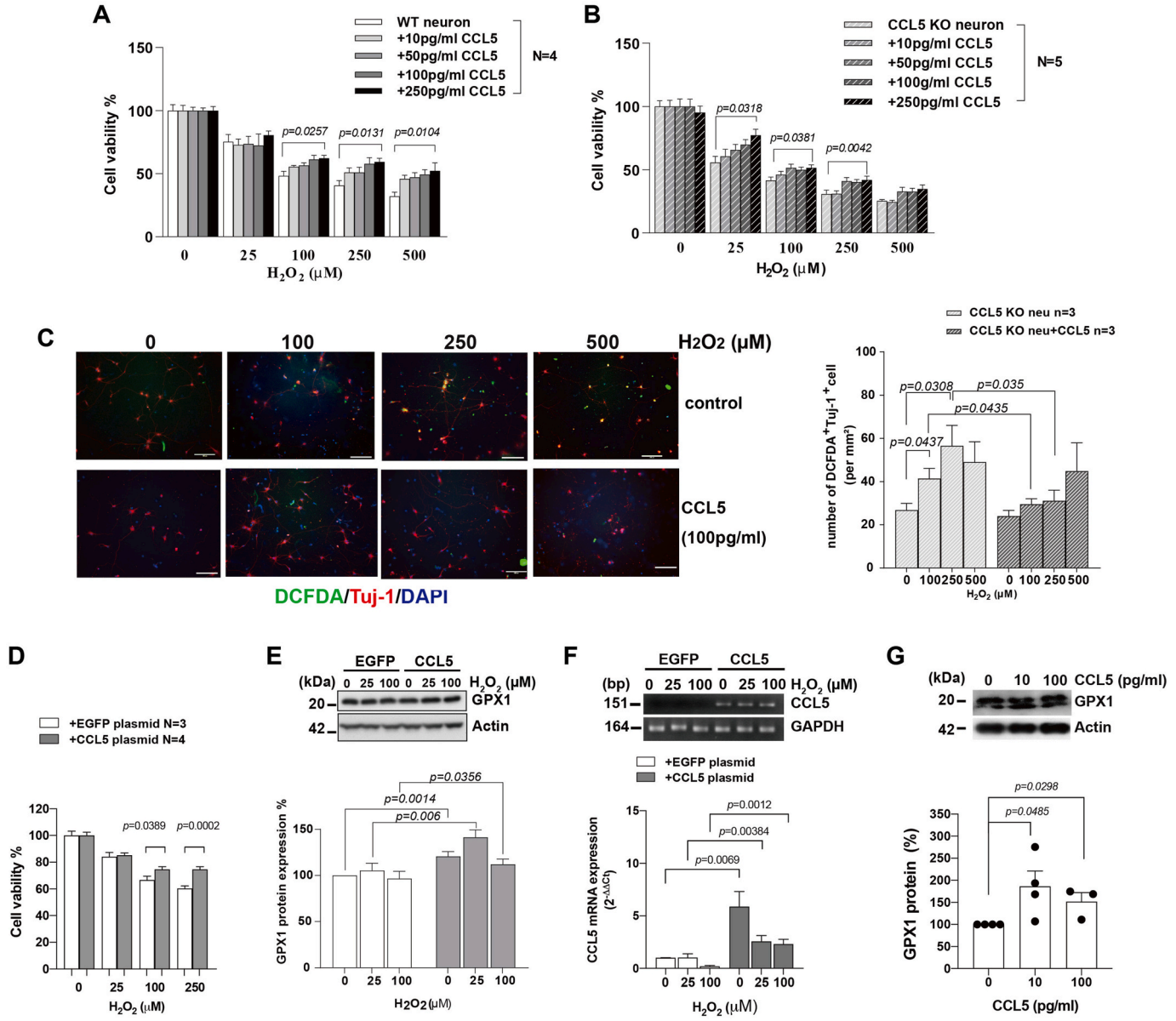

Fig. 5. CCL5 effects on cell viability, intracellular oxidative stress and GPX1 activation after H_2O_2 treatment. (A–B) Primary cortical neurons cultured from WT and CCL5-KO were treated with CCL5 (10 pg/ml, 50 pg/ml, 100 pg/ml and 250 pg/ml) for 30 min before H-$_2O_2$ treatment (0, 25, 250 and 500 μM). Cell viability was detected by MTT assay after 24 h (Data was analyzed by two-way ANOVA and presented as mean ± S.E.M.) (n = 5). (C) Representative images of DCFDA (green) and the neuron marker—Tuj-1 (red) labeling in CCL5 KO primary cortical neurons after 24hr treatment. The quantification of DCFDA labeled cells after CCL5 and H_2O_2 treatment. (Data was analyzed by *t*-test and presented as mean ± S.E.M.) (n = 3 in each group.) Scale bar = 100 μm in C. (D–E) SHSY5Y cells transfected with EGFP or CCL5 plasmids were treated with 0, 25, 100, 250 μM H_2O_2 for 24hr. (D) The viability of EGFP and CCL5-expressing cells was measured by MTT assay. (Data was analyzed by *t*-test and presented as mean ± S.E.M., N = 3–4) (E) Protein blots of GPX1 and GADPH in EGFP and CCL5-expressing SH5Y5 cells with H_2O_2 treatment. The quantification of GPX1 protein is shown below protein blots. (F) The CCL5 expression levels after transfection with EGFP or CCL5 plasmids. (G) The protein level of GPX1 in primary cultured neurons after treatment with recombinant CCL5. (Data was presented as mean ± S.E.M., N = 3–4.). (For interpretation of the references to color in this figure legend, the reader is referred to the Web version of this article.)

2.6. N-acetyl cysteine (NAC), a GPX precursor, reduced tissue ROS and prevented memory loss in CCL5-KO mice after mild brain trauma

In order to further define the mechanism of CCL5 in protecting neurons, 5 mg/kg or 20 mg/kg of NAC, a precursor of GPX1, was injected into mice after weight drop-induced brain trauma. TBI mice were injected with saline as controls (Fig. 6A. Details in the Material and Methods). We first tested the effects on memory before trauma. The primary latency was similar in different groups before trauma, but increased in saline treated KO mice after trauma (KO-TBI group) in the 2 days recall test. In contrast, mice receiving NAC after trauma showed a lower primary latency; moreover, the primary latency in the NAC 20 mg/kg group was similar in that seen in the sham group (Fig. 6B). New learning and memory training in the BM at 4 dpi was significantly improved by both 5 mg/kg and 20 mg/kg NAC treatment compared to the saline-treated TBI group (Fig. 6C); memory recall was also significantly improved with 20 mg/kg NAC (Fig. 6D). Hippocampal ROS was also reduced by both 5 mg/kg and 20 mg/kg NAC treatment (Fig. 6E). The number of oxidative stressed neurons (hypoxyprobe$^+$ and NeuN$^+$ cells) was also reduced in NAC-treated mouse hippocampus after trauma (Fig. 6F and G). In addition, the GPX1 mRNA level in mouse hippocampus was increased by the higher level by NAC treatment (Figs. 6H

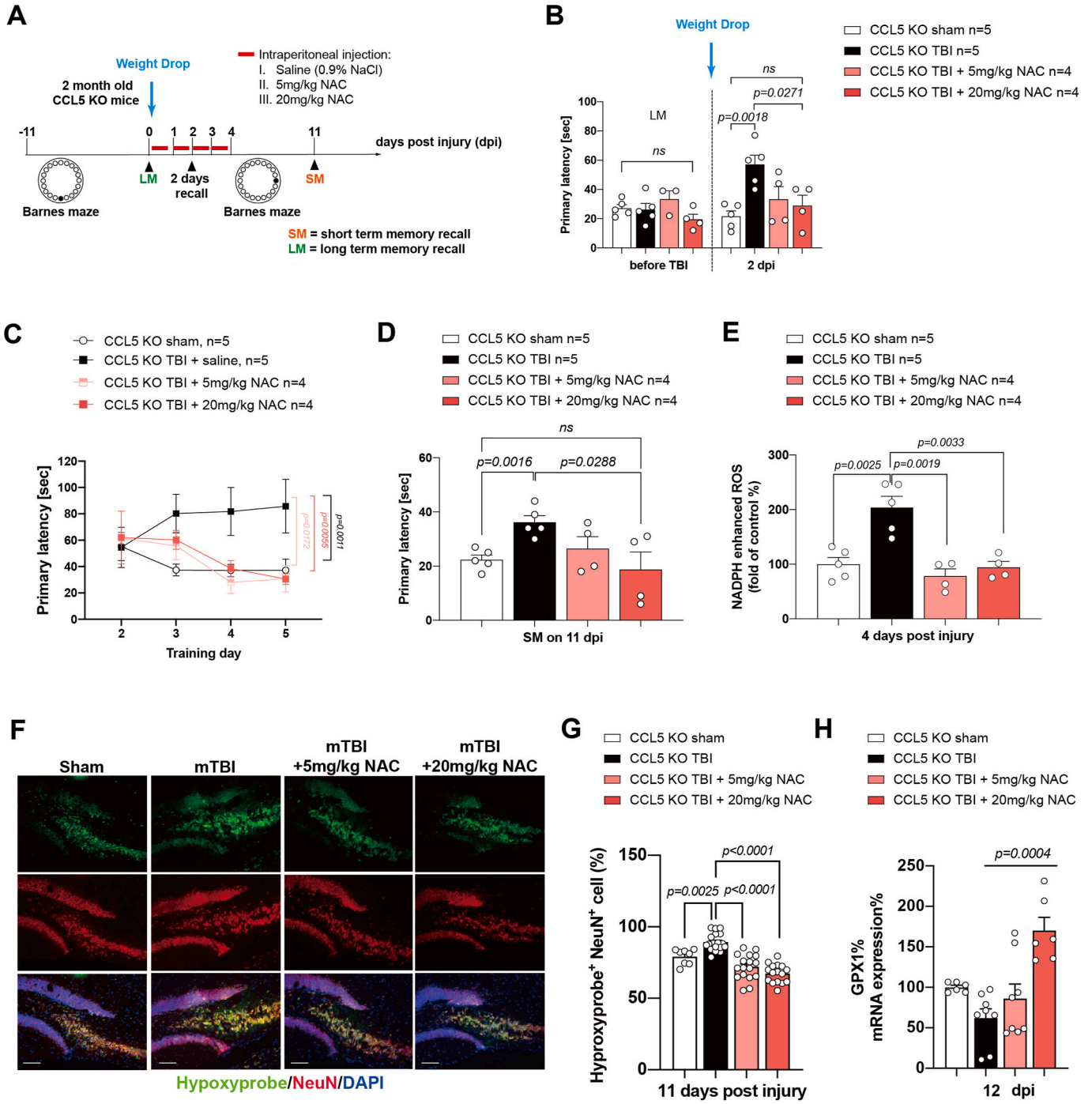

Fig. 6. NAC treatment improved memory impairment seen in CCL5 KO mice after mTBI. (A) Experimental design for NAC treatment in CCL5-KO mice after mild TBI induction and the Barnes maze test. (B) The primary latency of KO mice long-term memory recall (LM) before injury, and after injury with a 2 days recall memory test in sham, TBI, and TBI plus NAC treatment (5 mg, 20 mg) after weight-drop-induced mild TBI. (C) New Barnes maze learning and memory training progression in 4 groups 4 days after injury. (D) The primary latency in the short-term recall memory test (SM) between 4 groups. (F) The intracellular oxidative stress in sham, TBI and TBI plus NAC treatment in KO mouse hippocampus. (G) The quantification of hypoxyprobe and NeuN positive cells (hypoxyprobe^{+}NeuN^{+}) in the different groups. (H) The mRNA expression of GPX1 after TBI in 4 groups.

and 20 mg/kg).

2.7. CCL5 increased GPX1 mRNA transcription, reduced tissue ROS, and prevented memory loss in CCL5-KO mice after mild brain trauma

Finally, we used recombinant CCL5 protein to perform rescue experiments *in vivo*. Recombinant CCL5 was administered through an intranasal (i.n.) route, via the rostral migratory stream, into mouse ventricles after weight drop-induced brain trauma. Recombinant CCL5 was conjugated with Alexa-594 dye to track the brain distribution after i.n. delivery (Supl. Fig. 6B). PBS was used as a control (Supl. Fig. 6A); the study design is shown in Fig. 7A, which is similar to the NAC study. The primary latency was similar in different groups before trauma and increased in PBS treated TBI KO mice (KO-TBI + PBS group) in the 2 days recall test. Interestingly, mice receiving CCL5 showed a lower primary latency which was similar to that before trauma (Fig. 7B). New

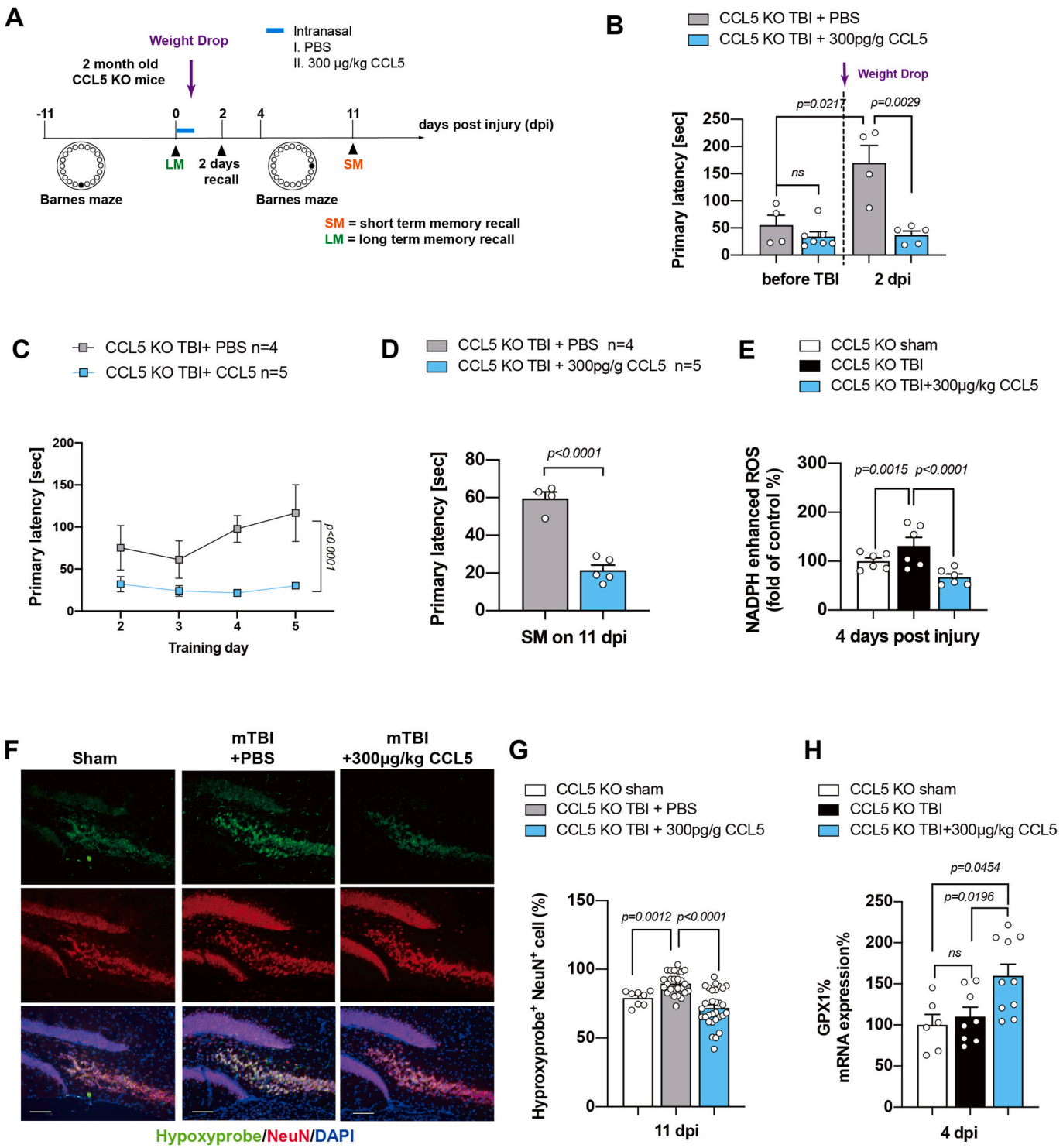

Fig. 7. CCL5 increased GPX1 mRNA transcription reduced cellular ROS and improved memory impairment seen in CCL5 KO mice after mTBI. (A) Experimental design for CCL5 treatment in CCL5-KO mice after mild TBI induction and the Barnes maze test. (B) The primary latency of KO mice before injury, and after injury with a 2 days recall memory test in mice with PBS treatment and CCL5 administration (300 μg/kg) after weight-drop induced mild TBI. (C) New Barnes maze learning and memory training progression in 2 treatment groups (4 days) after injury. (D) The primary latency in the short-term recall memory test (SM) between 2 treatments. (F) The intracellular oxidative stress in TBI sham, PBS and CCL5 treatment in KO mouse hippocampus. (G) The quantification of hypoxyprobe and NeuN positive cells (hypoxyprobe^{+}NeuN^{+}) in the different groups. (H) The mRNA expression of GPX1 after TBI with CCL5 treatments.

learning and memory training was significantly better in the CCL5 treated group compared to the PBS treated TBI group (Fig. 7C); the short-term memory recall test was also improved (Fig. 7D). Hippocampal ROS was significantly reduced by CCL5 treatment (Fig. 7E); the number of OS neurons (hypoxyprobe^{+} and NeuN^{+} cells) was also reduced in CCL5-treated mouse hippocampus after trauma (Fig. 7F and G). Importantly, the GPX1 mRNA levels in mouse hippocampus was also significantly enhanced by CCL5 after trauma (Fig. 7H).

In summary, we showed here that CCL5 is critical for antioxidant – GPX1 activation which reduces H_2O_2 from NADPH oxidase and protects

hippocampal neurons after TBI (Fig. 8A). Neurons lacking CCL5 generate more hydroxyl radicals which damage neurons probably through the Fenton reaction (Fig. 8B).

3. Discussion

We identified here a new function of CCL5 in antioxidant GPX-1 activation and protection of neurons from ROS damage after mild brain trauma. This CCL5 function further reduces astrogliosis, ROS generation through NADPH oxidase, neuronal degeneration, and significant memory impairment after mild brain trauma.

In previous studies NADPH oxidase activity increases within 1 h in neurons and a second increase is seen around 24–96 h after trauma. Interestingly, CCL5 mRNA is upregulated in the cortex immediately after injury and decreases 24–48 h after brain trauma which is parallel to elevated OS in brain tissue [10,11,23]. Many studies have shown the correlation between CCL5 and the NADPH oxidase response in immune cells' priming processes [24]; moreover NADPH oxidase is associated with CCL5 activation [25]. We also found lower NADPH oxidase activity in mice without CCL5 [15] which suggests removing CCL5 should reduce OS and protect neurons from NADPH oxidase damage after trauma. However, mice lacking CCL5 showed a failure to protect neurons from ROS damage but conversely had more OS in neurons and astrocytes after brain injury (Fig. 3E, Supl. Fig. 3A, C). One study found that CCL5 and its receptor CCR5 induce copper/zinc-superoxide dismutase (SOD-1) expression in macrophages [26]. In the current study, a reduction of SOD1 in CCL5-KO mouse hippocampus after injury (Fig. 4G) was found. More importantly, GPX1 failed to be activated after injury in CCL5-KO mice.

GPX enzyme families are the key to convert H_2O_2 into harmless H_2O and O_2. The level of GPX1 protein as well as CCL5 increased 4–7 days after injury in WT hippocampus tissue (Fig. 4F and Supl. Fig. 4A). We further found an enhancement of GPX1 protein together with overexpression of CCL5 in SHSY5Y cells (Fig. 5E) and recombinant CCL5 treatment in primary neurons (Fig. 5G) as well as after i.n. delivery of CCL5 into CCL5 KO mice (Fig. 7H). Treating mice with the GPX precursor – NAC shortly after injury for 3 days reduced neuronal oxidative stress and subsequent loss (Fig. 6). Delivery of CCL5 into mouse brain one time through i.n. at 1hr after injury also reduced oxidative stress and neuronal death (Fig. 7). Moreover, both NAC and CCL5 treatment improved hippocampal memory-cognition function (Fig. 6 B-D, and Fig. 7-D). Our data thus strongly support that CCL5 and GPX function as anti-oxidative stress and neuroprotection molecules after injury with a critical time window of post injury 1hr to 3 days.

Many studies have shown that Minocycline plus *N*-acetylcysteine (MINO plus NAC) together improved the cognition and memory in a rat mild controlled cortical impact (mCCI) model of traumatic brain injury. The combined treatment with MINO and NAC modulated the neuroinflammation status by increasing type 2 microglia specifically [7]. This treatment also promoted remyelination and improved cognition and memory performance in different animal behavioral tasks [27,28]. In the current study, we found an increase of inflammatory chemokines, specially IL-10, in WT mice but not in the CCL5-KO mice after brain injury. This inflammatory response was reduced after 7 days together with an improvement in animals' behavioral performance. Although there was a lower level of inflammation in the CCL5-KO mouse hippocampus in the first 7 days, more OS was found (Fig. 3); inflammation increased in KO mice after 7–14 days. These data suggest an importance of the balance between OS and inflammation starts during the first 3 days which subsequently determines the direction of neuron repair. Together, CCL5 might play a role in directing inflammatory status under OS soon after brain injury. These current findings provided an important mechanistic basis for our study of NAC in military personnel after blast injury in Iraq [5,6]. We found that NAC improved physical symptoms and cognitive function after blast injury with a critical time window of 24 h–72 h for drug administration after injury. Beyond 72 h, NAC was significantly less effective. Both MINO and NAC are Food and Drug Administration-approved drugs which allow them to be used in the clinic immediately.

The regulation and activation of CCL5 may thus correlate with injury progression and status. The function of CCL5 depends on the activation of different receptors such as CCR1, CCR3, CCR5 and GPR75. Previous studies found that treating mice with the CCL5's receptor antagonist, Maraviroc, protects neuron after stroke and severe TBI in animals [29]. Silencing CCR5 with short hairpin RNA (shRNA) in hippocampal CA1 and CA3 regions two weeks before injury, or with pharmacological

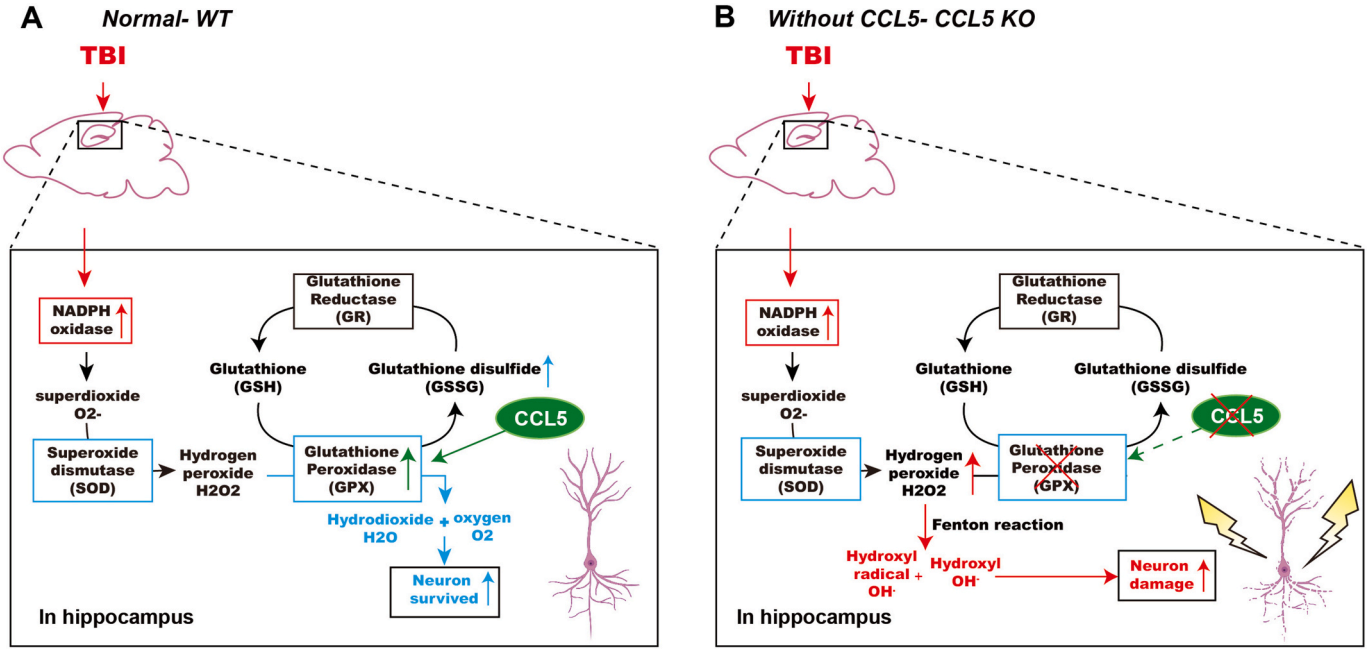

Fig. 8. Summary of CCL5 in GPX1 activation and neuron protection after brain injury. (A) Brain injury induces ROS generation in mouse hippocampus which can be scavenged by the SOD and GPX systems and increase neuron survival with the presence of CCL5. (B) Increased H_2O_2 produces hydroxyl radical (OH·) and hydroxy (OH^-) through the Fenton reaction and causes hippocampal neuron death in the absence of CCL5.

blockers such as Maraviroc and plerixafor, reduced the injured area and astrocytosis in mouse cortex [30,31]. It should be noted that the above studies involved severe brain damage in animals, whereas our study was performed with a mild brain injury protocol. The mechanisms and responses can be very different under these two conditions. Our study found more astrogliosis (Supl. Fig. 3A, C) oxidative stress (Fig. 3) and neuron loss (Fig. 2) in CCL5-KO mice after 1-month mild TBI. Neurons cultured from CCL5-KO mice were more sensitive and vulnerable to H_2O_2 induced oxidative stress, but the protective role of CCL5 was reduced when the H_2O_2 oxidative stress was higher than 500 μM (Fig. 5B, C and D).

Most brain injuries are mild and repetitive such as with vehicle accidents, American football, hockey [32] and blast during the war. We also found the protective dosages of CCL5 were lower than 500 pg/ml and the level of CCL5 in hippocampal tissue and blood was little increased in our mild TBI model (Supl. Fig. 4A and B); severe TBI might induce a higher level of CCL5, more than 1000 pg/ml release, and this may activate different signaling/functions. This also suggests very different roles and mechanisms for CCL5 in brain injury when damage is more severe. This dichotomy may involve differential dose-dependent neuroimmune effects.

To understand how to treat mild brain injuries is critical and urgent. From our study and others', different levels of severity of injury might have different neuronal damage mechanisms which require different treatments in the clinic. We found however that the first 1 h to 3 days post injury is a critical window for CCL5 and NAC - antioxidant activation and treatment for mild brain injury; CCR5/CXCR4 anti-inflammation related treatment as well might be more suitable for severe brain injury. This window time is similar to our clinical study in Iraq [6].

In conclusion, CCL5 has a unique function in antioxidant GPX-1 activation which reduces cellular ROS and inflammation induced - astrocytosis after mild brain injury. This function reduces further neuronal degeneration and memory impairment after mild brain traumatic injury.

4. Materials

Chemicals used in study were purchased from Sigma-Aldrich (Missouri, USA) and Merck (Darmstadt, Germany). Cell culture related media and reagents were purchased from Invitrogen/Thermo Fisher scientific (Massachusetts, U.S.).

5. Experimental model and methods

5.1. Animas and weight-drop model of mild TBI

Traumatic brain injury (TBI) studies were performed in accordance with protocols approved by the Institutional Animal Care and Use Committees of the Taipei Medical University (Protocol numbers: LAC-2015-0397; LAC-2019-0020; LAC-2019-0587). Male C57BL/6 mice from the National Laboratory Animal Center were used for wild type. Male B6.129P2-Ccl5^{tm1Hso}/J originally from Jackson Laboratories were bred and maintained by the National Laboratory Animal Center (CCL5-$^{-/-}$mice, Jackson Laboratory, Stock No: 005090). Mice were housed in groups of 3–5 per cage with free access to food and water on a 12:12-h light/dark cycle and with room temperature set at 25 °C. All the behavior tests in current study were also performed at 25 °C.

Mild TBI was induced by weight drop as previously described [33–36]. Briefly, 2-3-month-old WT or CCL5$^{-/-}$ mice were anesthetized with 2.5% isoflurane (Panion & BF biotech Inc.) with an air flow rate of 1.5–2.0 L/min for 2 min 15 s; subsequently the mouse was placed chest down on a foam sponge (dimensions: 18.5 cm × 7 cm × 8 cm) to support the head and body underneath a weight-drop device. The weight-drop device consisted of a hollow cylindrical tube (inner diameter 1.2 cm, 100 cm height) placed approximately 2 cm vertically over the center of the mouse's head. A 30 g weight (1 cm diameter, 5.2 cm height) was released down the tube and struck the mouse to induce mild TBI. Sham animals were anesthetized only. The unconsciousness times were measured after mice received impact until a righting reflex was seen.

For the rescue study, CCL5 KO mice were treated with NAC (A7250, Sigma-Aldrich) or recombinant mouse CCL5/RANTES Protein (478-MR-025, R&D system). NAC was dissolved in normal saline and a dosage of 5 mg/kg or 20 mg/kg was administered. One hour after mild TBI, CCL5 KO mice was treated daily by i.p., until 4dpi behavioral testing. At 2 dpi, NAC was injected after the memory recall test to avoid any NAC short term effects. CCL5 recombinant protein was diluted with PBS and given to CCL5 KO mice with a 300 μg/kg dosage by i.n., which is effective for non-invasive administration in to brain [37]. To track the location of CCL5 after i.n., CCL5 recombinant protein was labeled with the Alexa Fluor™ 594 Microscale Protein Labeling Kit (A30008, Invitrogen) as protocol. 24hr after TBI, mice were sacrificed, perfused and CCL5 immunostaining was performed with anti-CCL5 antibody (1:100, sc-365826, Santa Cruz biotechnology, Dallas, USA) and donkey anti-rabbit-488 (1:400, Invitrogen, A32790).

5.2. Behavioral tests

Neurologic function consisted of several behavioral tests - **Modified Neurological Severity Scores (mNSS):** mNSS indicated overall neuronal function including motor, sensory, reflex and balance in WT and CCL5 KO mice after mild TBI [38]. The parameters were graded as 0 to 18 (healthy score: 0; highest deficit score: 18). Memory performance consisted of Novel object recognition (NOR) and Barnes maze (BM) tests. All testing was analyzed via EthoVision ® XT (version 12, Noldus, Boston, MA, USA) software.

Novel object recognition test (NOR): The novel object recognition test is a common test to measure recognition memory in rodents [39]. Mice were randomly divided into four Groups 4, 7, 14- and 28-days post injury (dpi groups). Mice were habituated in a closed 57 cm × 57 cm box for one day, and then reintroduced into the box for 10 min with 2 identical objects placed at an equal distance in the box on the second day. 24 h later, one of the objects was replaced with one of the same size and color but with a different shape. Time spent exploring each object was measured by EthoVision ® XT. Memory was defined as a discrimination index percentage (DI%= (Time spent novel object-Time spent familiar object)/total exploration time × 100%). The combination of objects was same in different groups to avoid object shape as a confound. The apparatus was cleaned with ethanol between trials to avoid odor recognition.

Barnes maze: The Barnes maze test was performed as previously described [40]. The maze consisted of a white circular platform (92 cm of diameter) with equally spaced holes at 3, 6, 9 and 12 o'clock positions. Mice were familiarized in a dark cage for 30 min before the test. In day 1, mice were habituated to the escape box for 5 min and habituated to the maze for 6 min. Over the next 4 days, mice were placed in the center of the maze and allowed to feely explore for 6 min. When they arrived at the escape box or explored for a time over 6 min the training was stopped. The memory recall test was also performed as previously described [41]. The short-term memory and long-term memory recall tests were performed at 2 days and 7 days after the last day of Barnes maze training. Primary latency, distance moved, and percentages of target quadrant visits during training and memory recall tests were measured with the software as above. In pre-TBI Barnes maze (−11 dpi Barnes maze), mice underwent training and memory recall tests to confirm their ability to learn and remember. The 2-dpi memory recall test (the position of escape box was the same as for11dpi Barnes maze) indicated the original memory impairment in WT and CCL5 KO mice after TBI. The position of the escape box was changed at different days post injury.

Animals were sacrificed for the following cellular and molecular analysis no more than 24 h after behavior analysis. Thus, the molecular

analysis could be temporally correlated with the behavioral results.

5.3. FJC staining

Mice were anesthetized with Zoletil 50 (66F4, Virbac) and Rompum solution (PP1523, Bayer) and then perfused with 4% PFA; harvested brains were cryostat sectioned at 25 μm and processed for Fluoro-Jade C (FJC) staining (TR-100-FJ, Biosensis, USA) following the manufacturer's instructions. In short, brain tissues were mounted on gelatin coated slides and heated at 57 °C for 30 min. Tissue was rehydrated with serially diluted EtOH and H_2O then blocked with 0.06% $KMnO_4$ solution for 10 min. After blocking, tissues were incubated with 0.0001% FJC solution containing 1 μg/ml DAPI for 10 min. Tissues were dehydrated with Xylene. Images were acquired using a fluorescence microscope (STP6000, LEICA). FJC positive cells were analyzed by Imager J software (Version 1.53c, National Institutes of Health, USA).

5.4. Immunohistochemistry, and hypoxyloprobe co-labeling

Hypoxyprobe staining was performed at 1 and 7 days post injury for measurement of OS damage in hippocampus after TBI [42]. Before perfusion, the Hypoxyprobe solution (pimonidazole hydrochloride dissolved in 0.9% NaCl), a 60 mg/kg intraperitoneal injection, was administered to the animal. After 60 min, mice were perfused with 4% paraformaldehyde (PFA) in 0.1 M phosphate buffer. Harvested brain tissues were cryostat sectioned at 25 μm and processed for immunohistochemistry. Tissues were retrieved by 1% sodium bicarbonate in 0.1 M phosphate buffer at 30 min. After blocking in 3% BSA in PBSc/m, tissues were incubated with primary antibody at 4 °C overnight. The number of neurons, microglia and astrocytes were measured using rabbit antibodies to NeuN (Novus- NBP1-77686X, 1:200 dilution), Iba-1 (GeneTex, GTX101495, 1:1000 dilution) and GFAP (GeneTex, GTX108711, 1:1000 dilution). Anti-pimonidazole-FITC (1:100, Hypoxyprobe™ Plus kit, Biosensis) was used to show the Hypoxyprobe signal. Anti-NeuN or GFAP were co-labeled to indicate OS neurons and astrocytes. After washing away the primary antibody, tissues were incubated with donkey anti-rabbit-568 (1:400, Invitrogen, A10042) or donkey anti-rabbit-488 (1:400, Invitrogen, A32790) for 40 min at room temperature. Images were acquired by fluorescence microscope and analyzed with Imager J. Controls consisted of omission of primary antibody and counts were made by blinded observers.

5.5. NADPH oxidase activity assay

Basal ROS production and NADPH oxidase activity was studied at 4dpi, 7 dpi, 14 dpi and 28 dpi as previously described [4]. Basal ROS production were carried out in a final volume of 200 μl Krebs buffer (pH 7.4, 118.4 mM NaCl, 25 mM $NaHCO_3$, 11.7 mM glucose, 4.75 mM KCl, 1.2 mM $MgSO_4$, 2.5 mM $CaCl_2.2H_2O$, 1.2 mM KH_2PO_4) containing 50 μM lucigenin (Sigma-Aldrich, 2315971) in hippocampus tissue. The basal levels of ROS were detected for 50 s. NADPH oxidase activity was assayed by adding 50 μM NADPH after basal ROS detection. Counts per second (CPS) were measured by Triathler Multilabel Test (425-004, HIDEX, Turku, Finland) and normalized by wet weight of tissue (μg). NADPH oxidase activity was analyzed by the area under curve during a 350 s reaction. Data in TBI groups were normalized with the sham group to measure a fold change in NADPH oxidase activity.

5.6. Western blotting

Tissue or cells were lysed by RIPA buffer (#20-188, Millipore, USA) with protease and phosphatase inhibitor (78441, Thermo Scientific™, USA). Electrophoresis was performed with 10% Tris-HCl protein gel; 30 μg of total protein was loaded per lane. Gels were run and transferred to PVDF membrane by a Trans-Blot® Cell system (Bio-Rad). Protein membranes were blocked with blocking buffer (5% skim milk in Tris-buffered saline with 0.05% Tween 20, TBST) for 1 h at room temperature and then incubated with different primary antibodies including anti-actin (Millipore, MAB1501), GPX-1 (GeneTex, GTX116040), SOD-1 (GeneTex, GTX100659) and SOD-2 (GeneTex, GTX116093) overnight at 4 °C. Membranes were incubated with HRP-conjugated secondary antibodies (Goat anti-Mouse IgG-HRP, 115-035-003; Goat anti-Rabbit IgG-HRP, 111-035-003, from Jackson ImmunoResearch) for 1 h at room temperature after 3 washes with TBST. The protein blots were shown by the Clarity Western ECL Substrate kit (Bio-Rad, 1705061); the intensities were quantified by Image J software.

5.7. RNA isolation and real time quantitative PCR analysis

Tissue RNA was collected by TRIZOL (15596018, Invitrogen) and reverse transcripted into cDNA with the High-Capacity cDNA Reverse Transcription Kit (4368813, Applied Biosystems™). Quantitative PCR was conducted using iTaq Universal SYBR Green Supermix (Bio-Rad) with the StepOnePlus™ Real-Time PCR System (4376600, Applied Biosystems™, USA). Primer sequences were: ***GPX1***: Forward – 5′-CGTTTGAGTCCCAACATCTC-3'; reverse – 5′-CGTTCATCTCGGTGTAGTCC-3′, size: 199 bp. ***CCL5***: Forward – 5′-TGCTGCTTTGCCTACCTC-3'; reverse – 5′-CTTGAACCCACTTCTTCTCT-3′, size: 151 bp. ***IL-1β***: Forward –5′-GCACTACAGGCTCCGAGATGAAC-3'; reverse - 5′-TTGTCGTTGCTTGGTTCTCCTTGT-3′, product size: 147. ***IL-10:*** Forward –5′-GCTCTTACTGACTGGCATGAG-3'; reverse - 5′-CGCAGCTCTAGGAGCATGTG-3', product size: 105 bp. ***TNF-α***: Forward –5′-GGAACTGGCAGAAGAGGCACTC-3'; reverse - 5′-GCAGGAATGAGAAGAGGCTGAGAC-3', product size: 89 bp. **mouse *GADPH***: Forward - 5′-GTGTTCCTACCCCCAATGTGT-3'; reverse - 5′-AGAGTGGGAGTTGCTGTTGAAG-3′, size: 176 bp. **Human *GADPH***: Forward - 5′-CACAAGAGGAAGAGAGAGA-3'; reverse - 5′- CACAGGGTACTTTATTGATG -3′, size: 164 bp (for SHSY5Y human blastoma cell line). Expression of mRNAs was normalized with GADPH and calculated using the percentage of $2^{-}\Delta CT(TBI)/2\text{-}\Delta CT(sham)$.

5.8. GSH/GSSG activity assay

Glutathione concentration was measured by a Glutathione Colorimetric Assay Kit (K261, BioVision Inc, USA) [43]. Hippocampus tissue was homogenized with glutathione assay buffer (4μl/tissue weight (mg)) on ice. A 20 μl sample was mixed with 160 μl reaction mixture or reducing reaction mixture to detect total GSH and reduced GSH production respectively. For total GSH production, the sample was measured with an iMark microplate absorbance reader (Bio-Rad, USA) at 415 nm for 30 min. For reduced GSH, the sample was measured at 415 nm and normalized using a standard glutathione calibration curve.

5.9. Cell culture, transfection and cell viability assay

Primary neurons were cultured from C57BL/6 and $CCL5^{-/-}$ embryos at day 16.5–17 (E16.5–17) [44]. Embryonic brain tissues were digested with buffer (2 mg/ml papain, Worthington, LS003119) and 0.05% Trypsin-EDTA (Gibco, 25200-072) in Dulbecco's Modified Eagle Medium (DMEM, 12800-017, Gibco) for 14 min and seeded with plating medium (neurobasal medium, 21103-049, Gibco) containing 10% v/v heat-inactivated fetal bovine serum (FBS, 10437-028, Gibco), 1% v/v Antibiotic-Antimycotic (15240-062, Gibco), and 2 mM L-glutamine (25030, Gibco)). After a 2 h attachment, medium was replaced with complete medium (neurobasal medium contain 1% v/v N-2 supplement, 17502048, Gibco), 2% v/v B-27 supplement (17504044, Gibco), 1% v/v Antibiotic-Antimycotic and 2 mM L-glutamine). Half of the medium was replaced every 3 days. Recombinant CCL5/RANTES was administered at 4 days in culture with concentrations of 10, 50, 100 and 250 pg/ml. After 30 min, H_2O_2 (PanReac AppliChem, 131077) was administered with concentrations of 25, 50, 100, 250, 500 μM for 24 h. For the cell line study, SHSY5Y was transfected with CCL5 plasmids and EGFP

plasmids (#6084-1, Addgene, MA, USA) with Lipofectamine™ 2000 Transfection Reagent (11668019, Invitrogen). CCL5 plasmids were generated as previously described [44].Transfected cells were passed into 6-well/24-well plates and treated with the indicated H_2O_2 and CCL5 doses noted above for protein collection and MTT assays.

For cell viability analysis, cells were incubated with MTT solution (10 μg/ml, M6494. Invitrogen™) for 1 h. Subsequently, 200 μl DMSO was added to lyse the cells and the signal was read at 550 nm. Data was normalized to the 0 μM-adminisered group.

5.10. DCFDA labeling and immunocytochemistry staining

Primary neurons were seeded into 6-well plates with a density 5×10^5. At div 4, neurons were treated with 100 pg/ml CCL5 30 min before H_2O_2 treatment (0, 250, 500 μM). After 24 h, medium was removed and washed off with PBS. 10 mM DCFDA in PBS (D399, Invitrogen, USA) was added to the cells for 1hr and cells were then fixed with 4% PFA for 10 min and subsequently blocked with buffer containing 1 μg/ml DAPI for 30 min. Cells were incubated with primary antibody with neuronal cytoskeleton marker Tuj-1 (1:2000, MAB5564, Millipore, USA) at 4 °C overnight. Anti-mouse 568 (1:400, Invitrogen, USA) was used as the secondary antibody. Neurons were visualized using a fluorescence microscope and analyzed with Imager J software.

5.11. CCL5 ELISA assay

The levels of CCL5/RANTES in WT and CCL5 KO hippocampus were measured using the mouse CCL5/RANTES DuoSet ELISA kit (DY478, R&D System) following the manufacturer's protocol [44]. 96-well microplates were coated overnight with capture antibody at room temperature, followed by a 2 h incubation with 1%BSA in PBS for blocking and then washed with PBS containing 0.05% Tween 20 (wash buffer). 100 μl tissue samples or standards were added to microplates, incubated for 2 h at room temperature and then washed with wash buffer. Next, samples were incubated with biotin-conjugated detection antibody for 2 h and then with a 30 min incubation with streptavidin-HRP plus substrate for signal development. Microplate samples were measured with an absorbance reader at 450 nm. The level of CCL5 in each sample was calculated based on a standard curve prepared for the same experiment and normalized by protein concentration.

5.12. Statistical analysis

Statistical analysis was performed using GraphPad Prizm 8.0 (GraphPad Software, Dan Diego, CA, USA). An unpaired *t*-test was used to detect differences between two groups, One-way ANOVA was used to detect differences within the same group with a confidence interval of 95% and two-way ANOVA was used to detect multiple factors. The Bonferroni correction was used for any serial measurements. A p value < 0.05 was considered significant. All results are presented as mean ± SEM.

Funding

This work was supported by grants from Ministry of Science and Technology (MOST 105-2628-B-038-005-MY3; MOST 108-2320-B-038-025; MOST 109-2320-B-038-016) and Sunny Brain Tumor and Brain Disease Research and Development Fund to S.Y. Chou. Ministry of Science and Technology (MOST 108-2321-B-038-008) to YH Chiang, WC Chang and B Hoffer.

Author contributions

MH H performed most of the studies including animal studies, NADPH activity, ROS analysis and IHC experiments and cellular studies. MH H and CH Y established the ROS and NADPH assay. TH H, TJ K, and JY C helped with animal behavior measurements and analysis. YH C and WC C helped with the study plan. B. H. and SY C participated in study design and wrote the manuscript.

Declaration of competing interest

The authors declare that there is no conflict of interest. Correspondence and requests for materials should be addressed to SY Chou (sichou@tmu.edu.tw; sichou@gmail.com).

Appendix A. Supplementary data

Supplementary data to this article can be found online at https://doi.org/10.1016/j.redox.2021.102067.

References

[1] C. Angeloni, C. Prata, F.V. Dalla Sega, R. Piperno, S. Hrelia, Traumatic brain injury and NADPH oxidase: a deep relationship, Oxid. Med. Cell Longev. 2015 (2015) 370312.
[2] M.W. Ma, J. Wang, Q. Zhang, R. Wang, K.M. Dhandapani, R.K. Vadlamudi, D. W. Brann, NADPH oxidase in brain injury and neurodegenerative disorders, Mol. Neurodegener. 12 (1) (2017) 7.
[3] M.W. Ma, J. Wang, K.M. Dhandapani, R. Wang, D.W. Brann, NADPH oxidases in traumatic brain injury - promising therapeutic targets? Redox Biol. 16 (2018) 285–293.
[4] Q.G. Zhang, M.D. Laird, D. Han, K. Nguyen, E. Scott, Y. Dong, K.M. Dhandapani, D. W. Brann, Critical role of NADPH oxidase in neuronal oxidative damage and microglia activation following traumatic brain injury, PloS One 7 (4) (2012), e34504.
[5] K. Eakin, R. Baratz-Goldstein, C.G. Pick, O. Zindel, C.D. Balaban, M.E. Hoffer, M. Lockwood, J. Miller, B.J. Hoffer, Efficacy of N-acetyl cysteine in traumatic brain injury, PloS One 9 (4) (2014), e90617.
[6] M.E. Hoffer, C. Balaban, M.D. Slade, J.W. Tsao, B. Hoffer, Amelioration of acute sequelae of blast induced mild traumatic brain injury by N-acetyl cysteine: a double-blind, placebo controlled study, PloS One 8 (1) (2013), e54163.
[7] M. Haber, S.G. Abdel Baki, N.M. Grin'kina, R. Irizarry, A. Ershova, S. Orsi, R. J. Grill, P. Dash, P.J. Bergold, Minocycline plus N-acetylcysteine synergize to modulate inflammation and prevent cognitive and memory deficits in a rat model of mild traumatic brain injury, Exp. Neurol. 249 (2013) 169–177.
[8] B.J. Hoffer, C.G. Pick, M.E. Hoffer, R.E. Becker, Y.H. Chiang, N.H. Greig, Repositioning drugs for traumatic brain injury - N-acetyl cysteine and Phenserine, J. Biomed. Sci. 24 (1) (2017) 71.
[9] M.K. Ghiam, S.D. Patel, A. Hoffer, W.R. Selman, B.J. Hoffer, M.E. Hoffer, Drug repurposing in the treatment of traumatic brain injury, Front. Neurosci. 15 (2021) 635483.
[10] R. Sandhir, V. Puri, R.M. Klein, N.E. Berman, Differential expression of cytokines and chemokines during secondary neuron death following brain injury in old and young mice, Neurosci. Lett. 369 (1) (2004) 28–32.
[11] R. Stefini, E. Catenacci, S. Piva, S. Sozzani, A. Valerio, R. Bergomi, M. Cenzato, P. Mortini, N. Latronico, Chemokine detection in the cerebral tissue of patients with posttraumatic brain contusions, J. Neurosurg. 108 (5) (2008) 958–962.
[12] A. Helmy, K.L. Carpenter, D.K. Menon, J.D. Pickard, P.J. Hutchinson, The cytokine response to human traumatic brain injury: temporal profiles and evidence for cerebral parenchymal production, J. Cerebr. Blood Flow Metabol. 31 (2) (2011) 658–670.
[13] K. Lumpkins, G.V. Bochicchio, B. Zagol, K. Ulloa, J.M. Simard, S. Schaub, W. Meyer, T. Scalea, Plasma levels of the beta chemokine regulated upon activation, normal T cell expressed, and secreted (RANTES) correlate with severe brain injury, J. Trauma 64 (2) (2008) 358–361.
[14] H.Y. Kim, H.J. Cha, H.S. Kim, CCL5 upregulates IL-10 expression and partially mediates the antihypertensive effects of IL-10 in the vascular smooth muscle cells of spontaneously hypertensive rats, Hypertens. Res. 38 (10) (2015) 666–674.
[15] R. Ajoy, Y.C. Lo, M.H. Ho, Y.Y. Chen, Y. Wang, Y.H. Chen, C. Jing-Yuan, C. A. Changou, Y.C. Hsiung, H.M. Chen, T.H. Chang, C.Y. Lee, Y.H. Chiang, W. C. Chang, B. Hoffer, S.Y. Chou, CCL5 promotion of bioenergy metabolism is crucial for hippocampal synapse complex and memory formation, Mol. Psychiatr. (2021 Apr 30) 1–17, https://doi.org/10.1038/s41380-021-01103-3. Online ahead of print.
[16] B. Laffer, D. Bauer, S. Wasmuth, M. Busch, T.V. Jalilvand, S. Thanos, G. Meyer Zu Horste, K. Loser, T. Langmann, A. Heiligenhaus, M. Kasper, Loss of IL-10 promotes differentiation of microglia to a M1 phenotype, Front. Cell. Neurosci. 13 (2019) 430.
[17] A. Shemer, I. Scheyltjens, G.R. Frumer, J.S. Kim, J. Grozovski, S. Ayanaw, B. Dassa, H. Van Hove, L. Chappell-Maor, S. Boura-Halfon, D. Leshkowitz, W. Mueller, N. Maggio, K. Movahedi, S. Jung, Interleukin-10 prevents pathological microglia hyperactivation following peripheral endotoxin challenge, Immunity 53 (5) (2020) 1033–1049, e7.
[18] M.I. Kester, W.M. van der Flier, A. Visser, M.A. Blankenstein, P. Scheltens, C. B. Oudejans, Decreased mRNA expression of CCL5 [RANTES] in Alzheimer's disease blood samples, Clin. Chem. Lab. Med. 50 (1) (2012) 61–65.

[19] D. Tripathy, L. Thirumangalakudi, P. Grammas, RANTES upregulation in the Alzheimer's disease brain: a possible neuroprotective role, Neurobiol. Aging 31 (1) (2010) 8–16.
[20] J.K. Lee, E.H. Schuchman, H.K. Jin, J.S. Bae, Soluble CCL5 derived from bone marrow-derived mesenchymal stem cells and activated by amyloid beta ameliorates Alzheimer's disease in mice by recruiting bone marrow-induced microglia immune responses, Stem Cell. 30 (7) (2012) 1544–1555.
[21] A. Ignatov, J. Robert, C. Gregory-Evans, H.C. Schaller, RANTES stimulates Ca2+ mobilization and inositol trisphosphate (IP3) formation in cells transfected with G protein-coupled receptor 75, Br. J. Pharmacol. 149 (5) (2006) 490–497.
[22] H. Tokami, T. Ago, H. Sugimori, J. Kuroda, H. Awano, K. Suzuki, Y. Kiyohara, M. Kamouchi, T. Kitazono, R. Investigators, RANTES has a potential to play a neuroprotective role in an autocrine/paracrine manner after ischemic stroke, Brain Res. 1517 (2013) 122–132.
[23] D. Tweedie, H.K. Karnati, R. Mullins, C.G. Pick, B.J. Hoffer, E.J. Goetzl, D. Kapogiannis, N.H. Greig, Time-dependent cytokine and chemokine changes in mouse cerebral cortex following a mild traumatic brain injury, Elife 9 (2020).
[24] S. Ullevig, Q. Zhao, C.F. Lee, H. Seok Kim, D. Zamora, R. Asmis, NADPH oxidase 4 mediates monocyte priming and accelerated chemotaxis induced by metabolic stress, Arterioscler. Thromb. Vasc. Biol. 32 (2) (2012) 415–426.
[25] B. Cha, J.W. Lim, K.H. Kim, H. Kim, 15-deoxy-D12,14-prostaglandin J2 suppresses RANTES expression by inhibiting NADPH oxidase activation in Helicobacter pylori-infected gastric epithelial cells, J. Physiol. Pharmacol. 62 (2) (2011) 167–174.
[26] L. Qiu, L. Ding, J. Huang, D. Wang, J. Zhang, B. Guo, Induction of copper/zinc-superoxide dismutase by CCL5/CCR5 activation causes tumour necrosis factor-alpha and reactive oxygen species production in macrophages, Immunology 128 (1 Suppl) (2009) e325–e334.
[27] S.G. Abdel Baki, B. Schwab, M. Haber, A.A. Fenton, P.J. Bergold, Minocycline synergizes with N-acetylcysteine and improves cognition and memory following traumatic brain injury in rats, PloS One 5 (8) (2010), e12490.
[28] M. Haber, J. James, J. Kim, M. Sangobowale, R. Irizarry, J. Ho, E. Nikulina, N. M. Grin'kina, A. Ramadani, I. Hartman, P.J. Bergold, Minocycline plus N-acteylcysteine induces remyelination, synergistically protects oligodendrocytes and modifies neuroinflammation in a rat model of mild traumatic brain injury, J. Cerebr. Blood Flow Metabol. 38 (8) (2018) 1312–1326.
[29] M.T. Joy, E. Ben Assayag, D. Shabashov-Stone, S. Liraz-Zaltsman, J. Mazzitelli, M. Arenas, N. Abduljawad, E. Kliper, A.D. Korczyn, N.S. Thareja, E.L. Kesner, M. Zhou, S. Huang, T.K. Silva, N. Katz, N.M. Bornstein, A.J. Silva, E. Shohami, S. T. Carmichael, CCR5 is a therapeutic target for recovery after stroke and traumatic brain injury, Cell 176 (5) (2019) 1143–1157, e13.
[30] S. Liraz-Zaltsman, Y. Friedman-Levi, D. Shabashov-Stone, G. Gincberg, D. Atrakcy-Baranes, M.T. Joy, S.T. Carmichael, A.J. Silva, E. Shohami, Chemokine receptors CC chemokine receptor 5 and C-X-C motif chemokine receptor 4 are new therapeutic targets for brain recovery after traumatic brain injury, J. Neurotrauma 38 (14) (2021 Jul 15) 2003–2017.
[31] Y. Friedman-Levi, S. Liraz-Zaltsman, C. Shemesh, K. Rosenblatt, E.L. Kesner, G. Gincberg, S.T. Carmichael, A.J. Silva, E. Shohami, Pharmacological blockers of CCR5 and CXCR4 improve recovery after traumatic brain injury, Exp. Neurol. 338 (2021) 113604.
[32] T.B. VanItallie, Traumatic brain injury (TBI) in collision sports: possible mechanisms of transformation into chronic traumatic encephalopathy (CTE), Metabolism 100S (2019) 153943.
[33] R. Mychasiuk, A. Farran, M. Angoa-Perez, D. Briggs, D. Kuhn, M.J. Esser, A novel model of mild traumatic brain injury for juvenile rats, JoVE 94 (2014).
[34] B. Mouzon, H. Chaytow, G. Crynen, C. Bachmeier, J. Stewart, M. Mullan, W. Stewart, F. Crawford, Repetitive mild traumatic brain injury in a mouse model produces learning and memory deficits accompanied by histological changes, J. Neurotrauma 29 (18) (2012) 2761–2773.
[35] C.N. Bodnar, K.N. Roberts, E.K. Higgins, A.D. Bachstetter, A systematic review of closed head injury models of mild traumatic brain injury in mice and rats, J. Neurotrauma 36 (11) (2019) 1683–1706.
[36] L.S. Moye, M.L. Novack, A.F. Tipton, H. Krishnan, S.C. Pandey, A.A. Pradhan, The development of a mouse model of mTBI-induced post-traumatic migraine, and identification of the delta opioid receptor as a novel therapeutic target, Cephalalgia 39 (1) (2019) 77–90.
[37] C. Xiao, F.J. Davis, B.C. Chauhan, K.L. Viola, P.N. Lacor, P.T. Velasco, W.L. Klein, N.B. Chauhan, Brain transit and ameliorative effects of intranasally delivered anti-amyloid-beta oligomer antibody in 5XFAD mice, J. Alzheimers Dis. 35 (4) (2013) 777–788.
[38] J. Chen, Y. Li, L. Wang, Z. Zhang, D. Lu, M. Lu, M. Chopp, Therapeutic benefit of intravenous administration of bone marrow stromal cells after cerebral ischemia in rats, Stroke 32 (4) (2001) 1005–1011.
[39] F. Fernandez, W. Morishita, E. Zuniga, J. Nguyen, M. Blank, R.C. Malenka, C. C. Garner, Pharmacotherapy for cognitive impairment in a mouse model of down syndrome, Nat. Neurosci. 10 (4) (2007) 411–413.
[40] K. Gawel, E. Gibula, M. Marszalek-Grabska, J. Filarowska, J.H. Kotlinska, Assessment of spatial learning and memory in the Barnes maze task in rodents-methodological consideration, Naunyn-Schmiedeberg's Arch. Pharmacol. 392 (1) (2019) 1–18.
[41] F. Darcet, I. Mendez-David, L. Tritschler, A.M. Gardier, J.P. Guilloux, D.J. David, Learning and memory impairments in a neuroendocrine mouse model of anxiety/depression, Front. Behav. Neurosci. 8 (2014) 136.
[42] T. Noto, Y. Furuichi, M. Ishiye, N. Matsuoka, I. Aramori, S. Mutoh, T. Yanagihara, N. Manabe, Temporal and topographic profiles of tissue hypoxia following transient focal cerebral ischemia in rats, J. Vet. Med. Sci. 68 (8) (2006) 803–807.
[43] J.H. Cha, Q.M. Yu, J.S. Seo, Vitamin A supplementation modifies the antioxidant system in rats, Nutr. Res. Pract. 10 (1) (2016) 26–32.
[44] S.Y. Chou, J.Y. Weng, H.L. Lai, F. Liao, S.H. Sun, P.H. Tu, D.W. Dickson, Y. Chern, Expanded-polyglutamine huntingtin protein suppresses the secretion and production of a chemokine (CCL5/RANTES) by astrocytes, J. Neurosci. 28 (13) (2008) 3277–3290.